Spin-orbit coupling and spin-triplet pairing symmetry in Sr₂RuO₄

Zhiqiang Wang [1,2] Xin Wang [1] and Catherine Kallin[1]

[1]*Department of Physics and Astronomy, McMaster University, Hamilton, Ontario, Canada L8S 4M1*
[2]*James Franck Institute, University of Chicago, Chicago, Illinois 60637, USA*

Spin-orbit coupling (SOC) plays a crucial role in determining the spin structure of an odd parity psedospin-triplet Cooper pairing state. Here, we present a thorough study of how SOC lifts the degeneracy among different p-wave pseudospin-triplet pairing states in a widely used microscopic model for Sr₂RuO₄, combining a Ginzburg-Landau (GL) free energy expansion, a symmetry analysis of the model, and numerical weak-coupling renormalization group (RG) and random phase approximation (RPA) calculations. These analyses are then used to critically re-examine previous numerical results on the stability of chiral p-wave pairing. The symmetry analysis can serve as a guide for future studies, especially numerical calculations, on the pairing instability in Sr₂RuO₄ and can be useful for studying other multiband spin-triplet superconductors where SOC plays an important role.

I. INTRODUCTION

Understanding an unconventional superconductor requires identifying and understanding both its superconducting order parameter symmetry and the pairing mechanism. The two are intimately connected. In Sr₂RuO₄, both of these are still not well understood. Early experiments, including muon spin relaxation [1], NMR [2], Polar Kerr effect [3] measurements, point toward a spin-triplet chiral p-wave pairing [4,5], which is a two-dimensional (2D) analog of the A phase of helium ³He [6] and is potentially useful for topological quantum computing [7,8].

However, it is difficult to reconcile the spin-triplet chiral p-wave picture with several other experiments [9]. Chiral edge currents have been predicted for the chiral p-wave pairing state but not detected [10,11]; splitting of the superconducting transition temperature T_c in the presence of an in-plane magnetic field or a uniaxial strain [12,13] is expected but not found. Recent NMR experiments [14,15] report a significant drop of the spin susceptibility in the superconducting phase measured in an in-plane magnetic field, which contradicts previous measurements [2] and suggest either spin-triplet helical or singlet pairing, although strong spin-orbit coupling [16,17] can complicate the interpretation of the experimental data.

Most theoretical studies [18,19] on the pairing mechanism are connected to spin or charge fluctuation mediated superconductivity, inspired by work on ³He [6]. However, spin fluctuations in Sr₂RuO₄ are complicated due to the multiorbital nature of its normal state. The normal state of Sr₂RuO₄ contains two quasi-1D α and β bands, derived mainly from the Ru t_{2g} d_{xz}, d_{yz} orbitals, and one quasi-2D band from the d_{xy} orbital. Although early on it was proposed that the superconductivity is dominated by one set of the three bands [20], more recent calculations suggest that superconductivity on the three bands is comparable and indicate that the three orbitals should

be treated simultaneously. A further complication in a microscopic analysis comes from the sizable spin-orbit coupling (SOC) which entangles the three orbital degrees of freedom with spin. The effect of SOC on the normal state Fermi surface (FS) has been emphasized previously in Ref. [16] and was recently found to be larger than previously thought [17]. However, the effect of SOC on the superconducting state is still poorly understood.

Understanding the effect of SOC on the superconducting phase is crucial to address the relative stability of chiral p-wave and helical p-wave pairing states. This is because in the absence of SOC, and in the weak-coupling limit, all spin-triplet p-wave pairing states are degenerate due to the unbroken spin rotation symmetry [21]. A mechanism to lift the degeneracy in the absence of SOC is to consider the spin fluctuation feedback effect due to the superconducting condensate itself, which spontaneously breaks the spin rotation symmetry and modifies the pairing interaction. This mechanism is responsible for the stability of the ³He A phase [6] and has been used to stabilize the chiral state in theories of Sr₂RuO₄. However, in a Ginzburg-Landau free energy expansion in terms of the superconducting order parameter near T_c, the feedback effect only appears at fourth-order; while the SOC effect can split T_c of different spin triplet states at quadratic order [21]. Therefore it is important to understand how the normal state SOC affects the stability of different pairing states.

The effect of SOC on the spin triplet pairing states in Sr₂RuO₄ has been studied previously in Refs. [21–28] semi-analytically to various degrees and included in different numerical calculations [18,29–31], using different models and approaches. However, a systematic and more complete treatment is lacking. Also, conflicting statements have been made regarding the degeneracy among different p-wave pairing states in the presence of SOC. In this paper, we present a complete Ginzburg-Landau free energy analysis of the

SOC effect on the superconducting state at quadratic order in the order parameter. Then we focus on a 2D three-band microscopic model with SOC and identify the terms that lift the degeneracy among different p-wave states based on a symmetry analysis of the model. The results are supplemented with numerical weak-coupling RG and RPA calculations [18,26]. This model has been adopted in different numerical calculations [18,24,26,27,29–33] under different approximations to determine the dominant pairing instability for Sr_2RuO_4. Our analysis shows that some of the previous numerical results obtained in certain parameter regimes are incorrect. Since our results are obtained largely based on symmetries of the model, they also apply beyond weak-coupling and provide a guide to future numerical calculations. Furthermore, some of the conclusions and analysis here can be applied to other multiband spin-triplet superconductors, where SOC is important for the pairing.

The rest of the paper is organized as follows. In Sec. II, a complete GL analysis of SOC effects on triplet states is presented. In Sec. III, we study the SOC induced GL free energy terms for Sr_2RuO_4 based on a widely studied 2D three-band microscopic model using analytical symmetry analyses and numerical weak-coupling RG calculations. In Sec. IV, we reexamine the chiral p-wave instability in Sr_2RuO_4, where we provide a new phase diagram calculated within the RPA for the microscopic model, and also generalize the 2D analysis to 3D. Sec. V contains our conclusions. Some details of the derivations are relegated to Appendices, including details on the extension of this work to 3D models of Sr_2RuO_4.

II. GENERAL GINZBURG-LANDAU ANALYSIS

In the presence of SOC, spin is not a good quantum number. However, time reversal and inversion symmetries still ensure a twofold degeneracy at each $\mathbf{k}$ point in the Brillouin zone, which can be used to define a pseudospin and to classify all possible pairing states into pseudospin singlet and triplet sectors. Here, we focus on pseudospin triplet p-wave pairing states.

For a general pseudospin triplet state the order parameter is a 2×2 matrix,

$$\hat{\Delta}(\mathbf{k}) \equiv \sum_{\mu=\{x,y,z\}} \sum_{j=\{x,y\}} d_j^\mu \, \sigma_\mu i\sigma_y \, \psi_j(\mathbf{k}). \qquad (1)$$

where σ_μ are Pauli matrices in pseudospin space; $\psi_j(\mathbf{k})$ are two basis functions in $\mathbf{k}$ space that transform like k_x and k_y under the D_{4h} point group.

In the absence of SOC, the GL free energy at quadratic order in the superconducting order parameter is

$$f_2^0 = \alpha^0(T) \left\langle \frac{1}{2} \mathrm{Tr}[\hat{\Delta}^\dagger(\mathbf{k})\hat{\Delta}(\mathbf{k})] \right\rangle_{\mathrm{FS}} \qquad (2a)$$

$$= \alpha^0(T) \sum_{\mu=\{x,y,z\}} \sum_{j=\{x,y\}} |d_j^\mu|^2, \qquad (2b)$$

where the superscript "0" indicates quantities defined for zero SOC. $\alpha^0(T) \propto (T_c^0 - T)$ and $\langle \cdots \rangle_{\mathrm{FS}}$ means averaged over the FS. The trace, $\mathrm{Tr}[\cdots]$, is performed in pseudospin space.

In general, the presence of SOC breaks both the full pseudospin SU(2) rotation and spatial D_{4h} symmetries. The

remaining symmetry group for a 2D model of Sr_2RuO_4 is $D_{4h}^{\hat{L}+\hat{S}} \otimes U(1)^C$, where $D_{4h}^{\hat{L}+\hat{S}}$ is the D_{4h} point group whose symmetry operations act simultaneously on the spatial $\mathbf{k}$ and pseudospin spaces. $U(1)^C$ is the charge U(1) gauge symmetry. Time-reversal and inversion symmetries are also assumed, although they might be spontaneously broken in the ground state. To derive the most general form of the GL free energy terms at quadratic order we consider all possible contractions of $(d_i^\mu)^* d_j^\nu$, viewed as a rank-4 tensor, such that the contracted results are a scalar that is invariant under all symmetry operations of $D_{4h}^{\hat{L}+\hat{S}} \otimes U(1)^C$. This leads to five terms in the GL free energy, which are tabulated in Table I. Details of the derivation can be found in Appendix A.

We can also write the SOC induced terms in terms of $\hat{\Delta}$. When the pseudospin rotation symmetry is broken, order parameter products other than $\hat{\Delta}^\dagger \hat{\Delta}$, such as $\hat{\Delta}^\dagger \sigma_i \Delta$ and $\hat{\Delta}^\dagger \sigma_i \Delta \sigma_j$, can also appear in Eq. (2a) [34]. Considering all such combinations that are invariant under the symmetry group $D_{4h}^{\hat{L}+\hat{S}} \otimes U(1)^C$ leads to the same conclusion that there are five independent terms in the GL free energy at quadratic order. The results can be found in Table IV of Appendix A.

Some of the terms in Table I have been identified previously [21–26,28], but Table I provides the most complete form of all possible SOC induced terms at quadratic order. These terms in general lift the degeneracy among different p-wave states, which belong to the five irreducible representations of the D_{4h} group and are classified in Table II. Depending on the symmetries of microscopic models, some of these terms may or may not appear. In the following, we focus on a particular 2D three-band interaction model [18], identify the

TABLE I. All possible SOC induced GL free energy terms at quadratic order in $\hat{\Delta}$ for pseudospin triplet pairing states of a 2D model. For 3D models there are additional terms, which can be found in Appendix C.

GL terms	Expressions in terms of d_j^μ
$f_2^{\mathrm{SOC},1}$	$|d_x^z|^2 + |d_y^z|^2$
$f_2^{\mathrm{SOC},2}$	$(d_x^x)^* d_y^y + (d_y^y)^* d_x^x$
$f_2^{\mathrm{SOC},3}$	$(d_y^x)^* d_x^y + (d_x^y)^* d_y^x$
$f_2^{\mathrm{SOC},4}$	$|d_x^x|^2 + |d_y^y|^2$
$f_2^{\mathrm{SOC},5}$	$|d_x^y|^2 + |d_y^x|^2$

TABLE II. Irreducible representations (irrep.) of the $D_{4h}^{\hat{L}+\hat{S}}$ point group. The order parameters are given for 2D models. Only the pseudospin triplet p-wave pairing states are considered. The first four irrep., $\{A_{1u}, A_{2u}, B_{1u}, B_{2u}\}$, give helical pairings that do not break time reversal symmetry; while the E_u irrep. supports two chiral states, $\hat{z}(k_x \pm ik_y)$, that spontaneously break time reversal symmetry.

irrep.	Order parameter
A_{1u}	$\mathbf{d}(\mathbf{k}) = \hat{x}k_x + \hat{y}k_y$
A_{2u}	$\mathbf{d}(\mathbf{k}) = \hat{x}k_y - \hat{y}k_x$
B_{1u}	$\mathbf{d}(\mathbf{k}) = \hat{x}k_x - \hat{y}k_y$
B_{2u}	$\mathbf{d}(\mathbf{k}) = \hat{x}k_y + \hat{y}k_x$
E_u	$\mathbf{d}(\mathbf{k}) = \hat{z}(k_x, k_y)$

SOC induced terms, and analyze how they affect the relative stability of different p-wave pairing states.

III. MICROSCOPIC DETERMINATION OF THE SOC INDUCED TERMS

We consider the microscopic model Hamiltonian,

$$H = H_K + V, \tag{3}$$

where H_K is the kinetic energy part that gives rise to the normal state Fermi surfaces, and V is the interaction. In addition to hopping terms, H_K contains a SOC term, which, written in $\mathbf{k}$ space, is

$$2\eta \mathbf{L} \cdot \mathbf{S} = \eta \sum_{\ell,m,n=1,2,3} i\epsilon_{\ell mn} c^\dagger_{\mathbf{k},m,s} \sigma^\ell_{ss'} c_{\mathbf{k},n,s'}, \tag{4}$$

where $\{1, 2, 3\} = \{d_{yz}, d_{xz}, d_{xy}\}$ orbitals, and $\{s, s'\}$ are the actual spins, not the pseudospins to be defined below. $\epsilon_{\ell mn}$ is the fully antisymmetric tensor and η is the SOC strength. $c^\dagger$ (c) is the electron creation (annihilation) operator.

Following Ref. [18], we write H_K in the basis $\Psi(\mathbf{k}) = [c_{\mathbf{k},1,\uparrow}; c_{\mathbf{k},2,\uparrow}; c_{\mathbf{k},3,\downarrow}; c_{\mathbf{k},1,\downarrow}; c_{\mathbf{k},2,\downarrow}; c_{\mathbf{k},3,\uparrow}]^T$, such that it is block diagonal

$$H_K(\mathbf{k}) = \begin{pmatrix} H_{\uparrow\uparrow}(\mathbf{k}) & 0 \\ 0 & H_{\downarrow\downarrow}(\mathbf{k}) \end{pmatrix}, \tag{5}$$

where

$$H_{ss}(\mathbf{k}) = \begin{pmatrix} \epsilon_{yz}(\mathbf{k}) & g(\mathbf{k}) + is\eta & -s\eta \\ g(\mathbf{k}) - is\eta & \epsilon_{xz}(\mathbf{k}) & i\eta \\ -s\eta & -i\eta & \epsilon_{xy}(\mathbf{k}) \end{pmatrix}. \tag{6}$$

ϵ_{yz}, ϵ_{xz}, and ϵ_{xy} describe intraorbital hoppings; while $g(\mathbf{k})$ is the only interorbital hopping for a 2D model.

The interaction [18] we consider is a multiorbital on-site Kanamori-Hubbard type interaction

$$V = \frac{U}{2} \sum_{i,a} n_{i,a,\uparrow} n_{i,a,\downarrow} + \frac{U'}{2} \sum_{i,a\neq b,s,s'} n_{i,a,s} n_{i,b,s'}$$

$$+ \frac{J}{2} \sum_{i,a\neq b,s,s'} c^\dagger_{ias} c^\dagger_{ibs'} c_{ias'} c_{ibs}$$

$$+ \frac{J'}{2} \sum_{i,a\neq b,s\neq s'} c^\dagger_{ias} c^\dagger_{ias'} c_{ibs'} c_{ibs}. \tag{7}$$

$n_{i,a,s} \equiv c^\dagger_{i,a,s} c_{i,a,s}$ is the spin and orbital resolved electron density operator at site i. U (U') is the intraorbital (interorbital) repulsive Hubbard interaction. J is the Hund's coupling, and J' the pair hopping. The Hund's coupling term can be also written as [35] $-J \sum_{i,a\neq b}(\mathbf{S}_{i,a} \cdot \mathbf{S}_{i,b} + n_{i,a}n_{i,b}/4)$, where $\mathbf{S}_{i,a}$ is the orbital resolved electron spin vector operator at site i and $n_{i,a} = n_{i,a,\uparrow} + n_{i,a,\downarrow}$. The Kanamori-Hubbard interaction V is derived from the Coulomb interaction and is invariant under $SO(3)$ rotations in the t_{2g} d-orbital space, provided $J' = J$ and $U' = U - 2J$ [35]. Crystal field splitting in Sr_2RuO_4 in general lowers the symmetry of the interaction in the orbital space, which, however, does not affect our following discussions. Each of the four terms of V is SU(2) spin rotational invariant. The repulsive V can give rise to Cooper pairing instabilities in non-s-wave channels [36].

A. Hamiltonian in the pseudospin basis

Using $a^\dagger_{i,a,\sigma}$ ($a_{i,a,\sigma}$) for electron creation (annihilation) operators with the pseudospin σ and orbital a at site i, we define

$$(a^\dagger_{i,1,\sigma}, a^\dagger_{i,2,\sigma}, a^\dagger_{i,3,\sigma}) \equiv (c^\dagger_{i,1,\sigma}, c^\dagger_{i,2,\sigma}, c^\dagger_{i,3,\bar\sigma}), \tag{8}$$

where $\bar\sigma = \downarrow (\uparrow)$ if $\sigma = \uparrow (\downarrow)$. Written in the pseudospin basis, $\widetilde\Psi(\mathbf{k}) = [a_{\mathbf{k},1,\uparrow}; a_{\mathbf{k},2,\uparrow}; a_{\mathbf{k},3,\uparrow}; a_{\mathbf{k},1,\downarrow}; a_{\mathbf{k},2,\downarrow}; a_{\mathbf{k},3,\downarrow}]^T$, the kinetic energy part $H_K(\mathbf{k})$ remains the same as in Eq. (6), whose $H_{\uparrow\uparrow}$ ($H_{\downarrow\downarrow}$) block can be identified with pseudospin $\uparrow$ ($\downarrow$).

Rewriting the interaction V in Eq. (7) in terms of $\{a^\dagger, a\}$ and denoting the new interaction by $\widetilde V$, we have

$$\widetilde V = \widetilde V_U + \widetilde V_{U'} + \widetilde V_J + \widetilde V_{J'}, \tag{9}$$

where

$$\widetilde V_U = \frac{U}{2} \sum_{i,a} n_{i,a,\uparrow} n_{i,a,\downarrow}, \tag{10a}$$

$$\widetilde V_{U'} = \frac{U' - J/2}{2} \sum_{i,a\neq b,\sigma,\sigma'} n_{i,a,\sigma} n_{i,b,\sigma'}, \tag{10b}$$

$$\widetilde V_J = -J \sum_i \left\{ \sum_{a\neq b} \mathbf{S}_{i,a} \cdot \mathbf{S}_{i,b} - 2 \sum_{a=\{1,2\}} \left[S^y_{i,a} S^y_{i,3} + S^z_{i,a} S^z_{i,3} \right] \right\}, \tag{10c}$$

$$\widetilde V_{J'} = \frac{J'}{2} \sum_{i,\sigma\neq\sigma'} \left\{ \sum_{a\neq b=\{1,2\}} - \sum_{a\neq b=\{2,3\}} - \sum_{a\neq b=\{1,3\}} \right\} a^\dagger_{ia\sigma} a^\dagger_{ia\sigma'} a_{ib\sigma'} a_{ib\sigma}. \tag{10d}$$

In these equations, all operators are in terms of $\{a^\dagger, a\}$: $n_{i,a,\uparrow} = a^\dagger_{i,a,\uparrow} a_{i,a,\uparrow}$, etc. In the following, we identify the terms in the Hamiltonian $H_K + \widetilde V$ that breaks the pseudospin rotational symmetry.

B. Degeneracy at $g(\mathbf{k}) = J = J' = 0$

Although the presence of H_{SOC} breaks spin rotation symmetry in the normal state, it does not necessarily lead to a symmetry breaking in the pseudospin space and, therefore, the degeneracy among different pseudospin triplet p-wave pairing states may remain intact. In the current model, this is the case when both $g(\mathbf{k}) \equiv 0$ and $J = J' = 0$. This has been pointed out previously in Ref. [24] by a direct expansion of the effective interaction in the Cooper pairing channel in terms of the SOC constant η up to quadratic order. Here, we provide a proof purely based on symmetry.

First notice that H_K can be brought into a pseudospin SU(2) invariant form by the following unitary transformation (written in the $\mathbf{k}$ space)

$$\mathcal{U}: \{a^\dagger_{\mathbf{k},1,\downarrow}, a_{\mathbf{k},1,\downarrow}\} \rightarrow \{-a^\dagger_{\mathbf{k},1,\downarrow}, -a_{\mathbf{k},1,\downarrow}\}, \tag{11}$$

if there is no interorbital hopping term, i.e., $g(\mathbf{k}) \equiv 0$ in Eq. (6). In this case, under the $\mathcal{U}$ transformation,

$$\widetilde H_K \equiv \mathcal{U}^\dagger H_K \mathcal{U} = H_{\uparrow\uparrow} \otimes \sigma_0, \tag{12}$$

where σ_0 is the identity matrix in the pseudospin space.

When $J = J' = 0$, the $\mathcal{U}$ transformation leaves $\widetilde{V}$ in Eq. (9) unchanged, which is pseudospin SU(2) rotational invariant since $\widetilde{V}$ and V share the same form. Therefore, if both $g(\mathbf{k}) \equiv 0$ and $J = J' = 0$, the whole microscopic Hamiltonian after the $\mathcal{U}$ transformation,

$$\widetilde{H} = \widetilde{H}_K + \widetilde{V}, \tag{13}$$

is pseudospin SU(2) invariant. Consequently, all p-wave pseudospin triplet pairing states resulting from the microscopic Hamiltonian are degenerate. This conclusion does not depend on how the microscopic model is treated, i.e., whether the pairing states are calculated in weak-coupling RG [18], RPA [29,30], or other methods.

C. SOC induced terms due to finite $g(\mathbf{k})$ but with $J = J' = 0$

When $g(\mathbf{k}) \neq 0$, after the $\mathcal{U}$ transformation, the kinetic energy part of the Hamiltonian can be written as $\widetilde{H}_K + \delta\widetilde{H}_K$ with $\widetilde{H}_K$ given in Eq. (12) and

$$\delta\widetilde{H}_K(\mathbf{k}) \equiv 2g(\mathbf{k})\{S_{12}^z(\mathbf{k}) + \text{H.c.}\}, \tag{14}$$

where $S_{12}^z(\mathbf{k}) \equiv 1/2 \sum_{\sigma,\sigma'} a_{\mathbf{k},1,\sigma}^\dagger \sigma_{\sigma,\sigma'}^z a_{\mathbf{k},2,\sigma'}$ is the interorbital pseudospin operator along the z direction. For $g(\mathbf{k})$, to be specific, we consider the nearest-neighbor interorbital hybridization as in Ref. [18], $g(\mathbf{k}) = -4t''' \sin k_x \sin k_y$, where t''' is the corresponding hopping integral.

Clearly, $\delta\widetilde{H}_K(\mathbf{k})$ breaks the full pseudospin rotational symmetry. It contributes to the GL free energy a term which, to the first order in t'''/t, is

$$\delta\mathcal{F} = \langle\delta\widetilde{H}_K(\mathbf{k})\rangle = a_2\left[f_2^{\text{SOC},2} - f_2^{\text{SOC},3}\right]. \tag{15}$$

$a_2 \propto t'''/t$, and the expressions of $f_2^{\text{SOC},2}$ and $f_2^{\text{SOC},3}$ are given in Table I. The average $\langle\cdots\rangle$ is performed in a mean-field p-wave pairing state obtained at $t''' = 0$ and over the $\mathbf{k}$ space. In arriving at this equation, we have used: (1) because of the $\sin k_x \sin k_y$ dependence in $g(\mathbf{k})$, only $(d_x^\mu)^* d_y^\nu$ type terms can appear in $\delta\mathcal{F}$ so that $\langle\cdots\rangle$ does not vanish after the $\mathbf{k}$ average; (2) $\delta\widetilde{H}_K(\mathbf{k})$ has a remaining symmetry in the pseudospin space; it is invariant under pseudospin rotations about the z axis. Written in terms of the components of the $\hat{\Delta}$ matrix, $\delta\mathcal{F} = a_2(-i/2)\{\Delta_{\uparrow\uparrow,x}\Delta_{\uparrow\uparrow,y}^* - \Delta_{\downarrow\downarrow,x}\Delta_{\downarrow\downarrow,y}^* - \text{c.c.}\}$. The subscript '$x$' indicates that the quantity transforms as k_x under the spatial D_{4h} group. This term has been identified in Refs. [24,28] using a quite different approach. Our derivation makes the microscopic symmetry origin of the term manifest.

Since $\delta\mathcal{F}$ in Eq. (15) preserves the pseudospin rotation symmetry in the xy plane, it splits the four p-wave helical states into two groups, $\{A_{1u}, A_{2u}\}$ and $\{B_{1u}, B_{2u}\}$. The two states in each group are related to each other by a fourfold pseudospin rotation about z. To leading order in t'''/t, the splitting of T_c between the two groups is $\delta T_c \propto |a_2| \propto |t'''|/t$. Since $\delta\mathcal{F}$ does not have any term that splits chiral states from helical states, the transition temperature of the chiral states, $T_c^{E_u}$, stays half way in between that of the two helical state groups, $T_c^{A_{1u}/A_{2u}}$ and $T_c^{B_{1u}/B_{2u}}$. We confirm these conclusions with a numerical weak-coupling RG calculation following Refs. [18,26]. The results are shown in Fig. 1. At larger t'''/t, the splitting between helical and chiral states has deviations from the linear dependence on t'''/t arising from higher
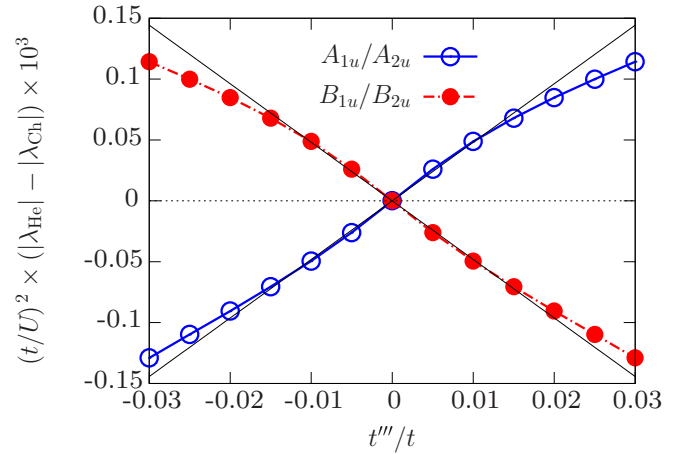

FIG. 1. Differences between eigenvalues of the effective two-particle interaction in the Cooper pairing channel computed within weak-coupling RG. Thin black lines are guides for the eye to show the linear behavior at small t'''/t. λ_{He} (λ_{Ch}) is the eigenvalue for p-wave helical (chiral) pairing states. The splitting, δT_c, of T_c between chiral and helical states is given by $\delta T_c/T_c \propto (|\lambda_{\text{He}}| - |\lambda_{\text{Ch}}|)$, to linear order in $\delta T_c/T_c$. The normal state band parameters, other than t''' and η, here and elsewhere, are identical to those in Ref. [18]. Here, we choose $\eta = 0.1t$ and $J/U = 0$.

order contributions of $\delta\widetilde{H}_K(\mathbf{k})$ to $\delta\mathcal{F}$, which lead to terms, $f_2^{\text{SOC},4} + f_2^{\text{SOC},5}$ and $f_2^{\text{SOC},1}$, in $\delta\mathcal{F}$. These terms leave the degeneracy in each of two helical state groups intact since the pseudospin rotational symmetry around z remains; however, they make the relation $T_c^{E_u} = \{T_c^{A_{1u}/A_{2u}} + T_c^{B_{1u}/B_{2u}}\}/2$ only an approximation. Since in Sr$_2$RuO$_4$, $|t'''|/t \sim \eta/t$ is small, we expect $T_c^{E_u} \approx \{T_c^{A_{1u}/A_{2u}} + T_c^{B_{1u}/B_{2u}}\}/2$ to hold, as seen in Fig. 1.

One conclusion of the above analysis is that the chiral pairing states are never stabilized by the t''' induced terms. A similar conclusion was obtained in Ref. [25] for a different interaction model within a mean-field analysis.

Since the relative stability between chiral and helical states will be affected by other SOC induced terms, which will be analyzed in detail in Sec. III D, it is important to understand the SOC dependence of $\delta\mathcal{F}$ in Eq. (15). Following Ref. [25], we go back to the original Hamiltonian before the $\mathcal{U}$ transformation in terms of actual spin. To linear order in η/t, the change of the GL free energy due to nonzero SOC is given by $\delta\mathcal{F} = 2\eta\langle\mathbf{L} \cdot \mathbf{S}\rangle$, where the average $\langle\cdots\rangle$ is evaluated in a mean field pairing state obtained at zero SOC. From the analysis of $\delta\widetilde{H}_K(\mathbf{k})$ in pseudospin space, we know that $\delta\mathcal{F}$ is invariant under pseudospin rotations about z; it is also invariant under actual spin rotations about z since the pseudospin and actual spin z directions are the same. Therefore, in $\langle\mathbf{L} \cdot \mathbf{S}\rangle$, $\langle L^x S^x + L^y S^y\rangle \equiv 0$. Hence,

$$\delta\mathcal{F} = 2\eta\langle L^z S^z\rangle = i\eta\{n_{12}^{\uparrow\uparrow} - n_{12}^{\downarrow\downarrow} - n_{21}^{\uparrow\uparrow} + n_{21}^{\downarrow\downarrow}\}, \tag{16}$$

where $n_{12}^{\uparrow\uparrow} \equiv \sum_i \langle c_{i1\uparrow}^\dagger c_{i2\uparrow}\rangle$ are the single-particle density matrices off-diagonal in the orbital index. At zero order in η, the mean field Hamiltonian for the chiral pairing states are symmetric with respect to spin $\uparrow \leftrightarrow \downarrow$. Consequently, the linear in η term in $\delta\mathcal{F}$ vanishes and $\delta\mathcal{F} \sim \mathcal{O}(\eta^2)$. On the other hand, for the four helical pairing states, $\delta\mathcal{F} \sim \mathcal{O}(\eta)$ in general, if

the superconducting order parameters on the α and β bands are not identically zero when $\eta = 0$. This linear dependence has been emphasized in Ref. [25].

We calculate the η dependence of $\delta\mathcal{F}$ for our model in weak-coupling RG. In the case of $J = 0$, we actually find that $\delta\mathcal{F} \propto (\eta/t)^2$ rather than $\propto \eta/t$. This comes from a complete decoupling between the $\alpha + \beta$ and γ bands when $J = J' = \eta = 0$, which makes all the density matrices in Eq. (16) identically zero and invalidates the above argument for the linear in η dependence (for details see Appendix B). When $J \neq 0$, the three bands are coupled and, indeed, we find the leading η/t dependence of $\delta\mathcal{F}$ linear, as shown in Fig. 5.

To summarize, the presence of $g(\mathbf{k})$ and η induces a pseudospin SU(2) symmetry breaking term in the GL free energy, given in Eq. (15), which lifts the degeneracy among different p-wave states. This term always favors helical states over the chiral states. It is invariant under the pseudospin rotations along z that preserves the degeneracy between A_{1u} and A_{2u}, and that between B_{1u} and B_{2u}. The splitting between the two helical state groups is $\delta T_c \propto t'''\eta/t$, to leading order in t'''/t and η/t. In the special case of $J = J' = 0$, the splitting is $\propto t'''\eta^2/t^2$. Interestingly, the necessary ingredients, t''' and η, for the splitting identified here are the same as those responsible for a spin Hall effect discussed in Ref. [37], suggesting that the two may be intimately connected.

D. SOC induced terms due to finite $J = J'$ but with $g(\mathbf{k}) \equiv 0$

In this section, we analyze the pseudospin rotational breaking terms due to finite J and η, while keeping $g(\mathbf{k}) \equiv 0$.

1. Pseudospin SU(2) breaking terms

When $J \neq 0$, applying the $\mathcal{U}$ transformation in Eq. (11) to $\widetilde{V}$ in Eq. (9) changes the form of $\widetilde{V}$ and leads to

$$\widetilde{\widetilde{V}} \equiv \mathcal{U}^\dagger \widetilde{V} \mathcal{U} = \widetilde{\widetilde{V}}_{\text{inv}} + \widetilde{\widetilde{V}}_J + \widetilde{\widetilde{V}}_{J'}, \tag{17}$$

where $\widetilde{\widetilde{V}}_{\text{inv}} = \mathcal{U}^\dagger (\widetilde{V}_U + \widetilde{V}_{U'}) \mathcal{U} = \widetilde{V}_U + \widetilde{V}_{U'}$ is still pseudospin SU(2) invariant. The other two terms are

$$\widetilde{\widetilde{V}}_J = \mathcal{U}^\dagger \widetilde{V}_J \mathcal{U} = -J \sum_i \left\{ \left[S_{i2}^x S_{i3}^x + S_{i1}^y S_{i3}^y + S_{i1}^z S_{i2}^z \right] \right.$$
$$\left. - \left[S_{i1}^x S_{i2}^x + S_{i1}^x S_{i3}^x + S_{i1}^y S_{i2}^y + S_{i2}^y S_{i3}^y + S_{i1}^z S_{i3}^z + S_{i2}^z S_{i3}^z \right] \right\}, \tag{18a}$$

$$\widetilde{\widetilde{V}}_{J'} = \mathcal{U}^\dagger \widetilde{V}_{J'} \mathcal{U} = \frac{J'}{2} \sum_{i,\sigma \neq \sigma'} \left\{ -\sum_{a \neq b = \{1,2\}} - \sum_{a \neq b = \{2,3\}} + \sum_{a \neq b = \{1,3\}} \right\}$$
$$\times a_{ia\sigma}^\dagger a_{ia\sigma'}^\dagger a_{ib\sigma'} a_{ib\sigma}. \tag{18b}$$

The $\mathcal{U}$ transformation shifts the SOC induced effect of spin rotational symmetry breaking from the kinetic energy part of the Hamiltonian to the interaction part. Note that the kinetic energy part becomes pseudospin SU(2) invariant after the transformation. Since each term of the original interaction V in Eq. (7) is SU(2) spin rotational invariant, we can identify the pseudospin SU(2) rotational symmetry breaking terms in

$\widetilde{\widetilde{V}}$ as

$$\delta\widetilde{\widetilde{V}} = -2J \sum_i \left[S_{i2}^x S_{i3}^x + S_{i1}^y S_{i3}^y + S_{i1}^z S_{i2}^z \right]$$
$$+ J' \sum_{i,\sigma \neq \sigma'} \sum_{a \neq b = \{1,3\}} a_{ia\sigma}^\dagger a_{ia\sigma'}^\dagger a_{ib\sigma'} a_{ib\sigma}. \tag{19}$$

In this equation the J' term alone does not lift the degeneracy among different p-wave pairing states. This can be proved within weak-coupling RG and RPA approximations by examining diagramatic contributions to helical and chiral states at each order in interaction. There is a one-to-one correspondence between the two contributions that contain J', if $J = 0$. This result is consistent with Ref. [24], where a direct perturbation, up to second order in both interaction and SOC, shows that the SOC induced terms to the effective interaction in the Cooper pairing channel necessarily depend on J when $g(\mathbf{k}) \equiv 0$. We have also verified the above conclusion in our numerical weak-coupling RG and RPA calculations. Therefore, within linear order in J ($= J'$), we can drop the J' term in Eq. (19).

2. GL free energy terms due to $\delta\widetilde{\widetilde{V}}$

$\delta\widetilde{\widetilde{V}}$ in Eq. (19) does not completely break the pseudospin SU(2) rotational symmetry. Mirror reflections about the xz and yz planes, denoted as $\mathcal{M}_{xz}^{\hat{S}}$ and $\mathcal{M}_{yz}^{\hat{S}}$ respectively, leave $\delta\widetilde{\widetilde{V}}$ invariant. This holds even if the J' term in Eq. (19) is taken into account. $\mathcal{M}_{xz}^{\hat{S}}$ and $\mathcal{M}_{yz}^{\hat{S}}$ are therefore symmetries of the whole microscopic Hamiltonian. In Table I, the only terms compatible with these symmetries are $f_2^{\text{SOC},1}$, $f_2^{\text{SOC},4}$, and $f_2^{\text{SOC},5}$. Therefore, in general, the GL free energy due to $\delta\widetilde{\widetilde{V}}$ is given by

$$\delta\mathcal{F} = a_1 f_2^{\text{SOC},1} + a_4 f_2^{\text{SOC},4} + a_5 f_2^{\text{SOC},5}$$
$$= \frac{2a_1 + a_4 + a_5}{4} \left[f_2^{\text{SOC},1} + f_2^{\text{SOC},4} + f_2^{\text{SOC},5} \right]$$
$$+ \frac{2a_1 - a_4 - a_5}{4} \left(f_2^{\text{SOC},1} - f_2^{\text{SOC},4} - f_2^{\text{SOC},5} \right)$$
$$+ \frac{a_4 - a_5}{2} \left(f_2^{\text{SOC},4} - f_2^{\text{SOC},5} \right), \tag{20}$$

where $\{a_1, a_4, a_5\}$ are three coefficients that shift the T_c away from T_c^0. In $\delta\mathcal{F}$, $(f_2^{\text{SOC},1} + f_2^{\text{SOC},4} + f_2^{\text{SOC},5})$ is trivial and shifts the T_c of all p-wave pairing states equally. To leading order in J/U, $\{a_1, a_4, a_5\} \propto J$.[1] $(f_2^{\text{SOC},1} - f_2^{\text{SOC},4} -$

---

[1]The leading order contribution to $\delta\mathcal{F}$ in a weak-coupling theory comes from a second order perturbation result, $\delta\mathcal{F} = \langle \widetilde{\widetilde{V}}_{\text{inv}} \widetilde{G}_4 \delta\widetilde{\widetilde{V}} \rangle$, which is second order in $\widetilde{\widetilde{V}}$ but first order in J/U. Here, $\langle \cdots \rangle$ means being averaged in a mean-field p-wave pairing state obtained at $J = 0$, and $\widetilde{G}_4$ is the four-point Green's function defined for the normal state Hamiltonian after the $\mathcal{U}$ transformation, $\widetilde{H}_K$ given in Eq. (12). Note that the first order perturbation contribution, $\langle \delta\widetilde{\widetilde{V}} \rangle$, is identically zero for a p-wave pairing state because the interaction $\delta\widetilde{\widetilde{V}}$ is purely on-site. However, because the pseudospin rotational symmetry property of $\delta\mathcal{F}$ is completely dictated by $\delta\widetilde{\widetilde{V}}$, in the main
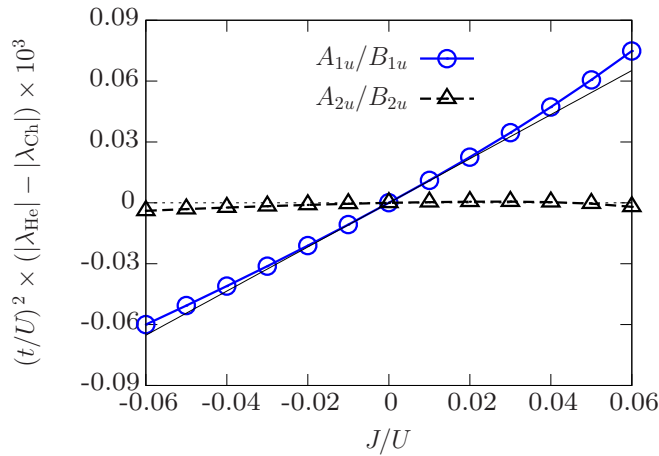
FIG. 2. J/U dependence of the splitting between helical and chiral p-wave pairing states in weak-coupling RG. $t''' = 0$ and $\eta = 0.1t$. The splitting is linear in J/U at small J/U. Note that the two helical states, $\{A_{2u}, B_{2u}\}$, are almost degenerate with the chiral state, which is accidental and not robust to band parameter changes.

FIG. 3. η/t dependence of the splitting between helical and chiral states in weak-coupling RG. $t''' = 0$ and $J/U = 0.06$. The splitting is $\propto (\eta/t)^2$ to leading order in η/t. Again, due to the near-degeneracy between the $\{A_{2u}, B_{2u}\}$ and chiral states for these band parameters, the quadratic dependence of the splitting in η/t is difficult to discern.

$f_2^{\mathrm{SOC},5}$) splits the chiral state away from helical ones, while $(f_2^{\mathrm{SOC},4} - f_2^{\mathrm{SOC},5})$ breaks the degeneracy among the four helical p-wave states, splitting them into two groups, $\{A_{1u}, B_{1u}\}$ and $\{A_{2u}, B_{2u}\}$. Within each group the two states are connected by $\mathcal{M}_{xz}^{\hat{S}}$ and $\mathcal{M}_{yz}^{\hat{S}}$, and therefore remain degenerate. In terms of the components of the order parameter matrix $\hat{\Delta}$, $f_2^{\mathrm{SOC},4} - f_2^{\mathrm{SOC},5} = (-1/2)\{[\Delta_{\uparrow\uparrow,x}^* \Delta_{\downarrow\downarrow,x} - \Delta_{\uparrow\uparrow,y}^* \Delta_{\downarrow\downarrow,y}] +$ c.c.$\}$. This term was identified in Refs. [24,28] using a direct expansion in the SOC, while our analyses here are based on symmetries of the model.

Again, it is important to understand the SOC dependence of $\delta\mathcal{F}$ in Eq. (20). For that we go back to the original Hamiltonian written in terms of the actual spin. As mentioned previously, the linear order in η/t contribution to the GL free energy comes from $\delta\mathcal{F} = 2\eta\langle \mathbf{L} \cdot \mathbf{S} \rangle$, where $\mathbf{S}$ is the actual spin operator, not pseudospin. However, $\langle \mathbf{L} \cdot \mathbf{S} \rangle \equiv 0$ because of the three remaining mirror reflection symmetries in the pseudospin space, $\{\mathcal{M}_{xz}^{\hat{S}}, \mathcal{M}_{yz}^{\hat{S}}, \mathcal{M}_{xy}^{\hat{S}}\}$, which imply the same symmetries for the actual spin, since the $\{x, y, z\}$ directions are identical in the pseudospin and actual spin spaces. On the other hand, these symmetries do not prohibit a second order in η/t term, $\delta\mathcal{F} \propto \langle (2\eta\, \mathbf{L} \cdot \mathbf{S})^2 \cdots \rangle$, where $\cdots$ here stands for η independent operators that have a dimension of energy inverse. Therefore, in Eq. (20), the GL expansion coefficients $\{a_1, a_4, a_5\} \propto (\eta/t)^2$ to leading order in η/t.

3. Numerical results

We confirm the above conclusions with weak-coupling RG calculations, where the details of the calculation follow Refs. [18,26]. Figure 2 shows the numerical results of the splitting between helical and chiral states as a function of J/U for fixed $\eta/t = 0.1$. At $J/U = 0$, all p-wave pairing states are
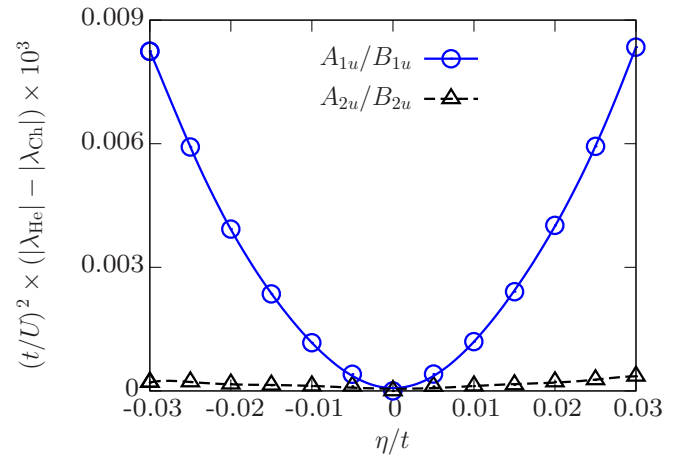
_____

text we simply focused on $\delta\widetilde{\widetilde{V}}$, rather than the more complicated $\widetilde{\widetilde{V}}_{\mathrm{inv}}\, \widetilde{G}_4\, \delta\widetilde{\widetilde{V}}$

degenerate, even though $\eta \neq 0$, consistent with the conclusion obtained in Sec. III B. At finite J/U, the degeneracy between chiral and helical states is lifted. The four helical states are split into two groups of two degenerate states. The splitting of T_c between the chiral states and the $\{A_{1u}, B_{1u}\}$ group is indeed $\propto J/U$ to leading order, as predicted. Interestingly, the other group, $\{A_{2u}, B_{2u}\}$, remains almost degenerate with the chiral states even at finite J/U, which is, however, not robust to changes of normal state band dispersions.

Figure 3 shows our weak-coupling RG results for the SOC dependence of $|\lambda_{\mathrm{He}}| - |\lambda_{\mathrm{Ch}}|$. Within numerical errors, $|\lambda_{\mathrm{He}}| - |\lambda_{\mathrm{Ch}}| \propto (\eta/t)^2$, in agreement with the above analytical analysis.

A summary of the main results obtained in this section is: finite $J = J'$ and η induce pseudospin rotational breaking terms in the GL free energy as given in Eq. (20), which lift the degeneracy among different p-wave pairing states. The splitting of T_c between different p-wave states is $\delta T_c \propto (J/U)\,\eta^2/t$, to leading order in J/U and η/t. The degeneracy between A_{1u} and B_{1u}, and that between A_{2u} and B_{2u}, remains due to pseudospin mirror reflection symmetries in the xz and yz planes. The terms in Eq. (20) can favor either chiral or helical states, depending on the magnitudes of the two coefficients, $(2a_1 - a_4 - a_5)/4$ and $(a_4 - a_5)/2$, which in turn depend on the normal state band structures. If $a_1 < \min\{a_4, a_5\}$, then $(2a_1 - a_4 - a_5)/4 < -|a_4 - a_5|/4$ and the chiral states are stabilized.

E. Results for both $g(\mathbf{k}) \neq 0$ and $J \neq 0$

When both $g(\mathbf{k})$ and $J = J'$ are nonzero, the SOC induced GL free energy is given by the sum of Eqs. (15) and (20). However, the GL free energy expansion coefficients for each $f_2^{\mathrm{SOC},j}$ are different from those in Eqs. (15) and (20) because of additional contributions that depend on both t''' and J. The degeneracy among all p-wave pairing states is lifted except the one between the two chiral states with opposite chirality
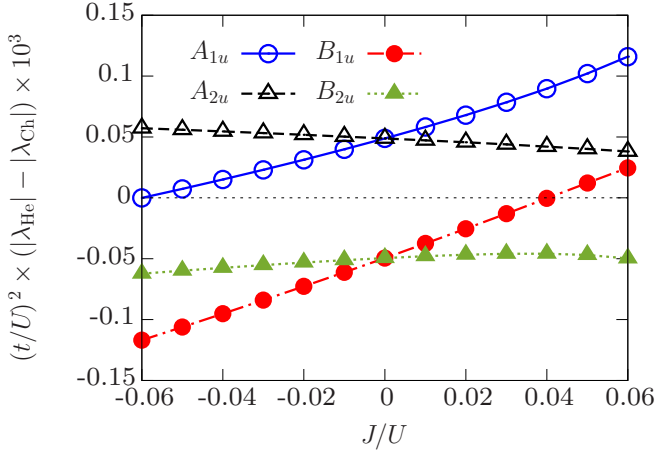
FIG. 4. J/U dependence of the splitting between different helical and chiral p-wave states. $t''' = 0.01t$ and $\eta = 0.1t$. The splitting at small J/U is dominated by the linear in t''' effect discussed in Sec. III C, which always stabilizes helical states.

within the E_u representation, as seen in Fig. 4. Because of the near-degeneracy seen in Fig. 2, the splitting between A_{2u} (or B_{2u}) and chiral states is dominated by the t''' term at small J/U. An implication is that, with both J and t''' present, the dominant p-wave pairing state in the small J/U and t'''/t parameter space regime will be always helical, rather than chiral, regardless of whether the splitting, $|\lambda_{\text{He}}| - |\lambda_{\text{Ch}}|$, for the other two helical states, $\{A_{1u}, B_{1u}\}$, is $\propto AJ/U$ with a positive slope $A > 0$, as seen in Fig. 4, or with $A < 0$. When t'''/t becomes larger, the splitting between $\{A_{2u}, B_{2u}\}$ and chiral states can pick up a significant J/U linear dependence because of cross dependent terms.

Some of the conclusions derived in Secs. III C and III D still hold when both t''' and J are present. For example, the leading SOC dependence of the splitting between different p-wave pairing states is linear due to the $g(\mathbf{k})$ induced terms, as shown in Fig. 5. These terms are $\propto t'''\eta/t^2$ to leading order in t'''/t.
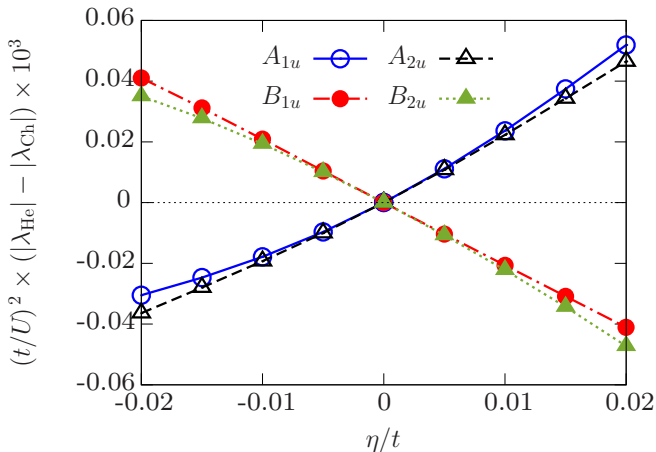

FIG. 5. η/t dependence of the splitting between helical and chiral p-wave states in weak-coupling RG. $t''' = 0.1t$ and $J/U = 0.11$. The leading SOC dependence is linear at small η/t.
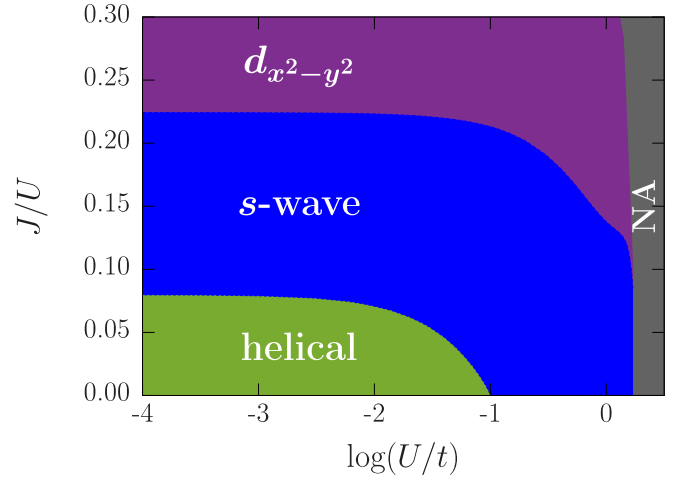

FIG. 6. Phase diagram obtained within RPA for different J/U and U/t. The RPA breaks down in the "NA" regime. The three intraorbital hoppings in Eq. (6) are $\epsilon_{xz(yz)}(\mathbf{k}) = -2t \cos k_{x(y)} - 2t^\perp \cos k_{y(x)} - \mu$, $\epsilon_{xy}(\mathbf{k}) = -2t'(\cos k_x + \cos k_x) - 4t'' \cos k_x \cos k_y - 2t''''(\cos 2k_x + \cos 2k_x) - \mu$. We choose the band parameters, $(t, t^\perp, t', t'', t''', t'''', \mu, \eta) = (1, 0.1, 0.8, 0.3, 0.05, -0.015, 1.075, 0.2)$, such that the resulting Fermi surfaces fit recent ARPES data [17].

IV. STABILITY OF CHIRAL p-WAVE PAIRING

The analysis of Sec. III shows that, within the current 2D three-band model with an on-site Kanamori-Hubbard interaction, the dominant pairing is always helical, rather than chiral, at small J/U and U/t where p-wave pairing is favored within the weak-coupling approximation [18,29,31]. On the other hand, at large J/U, pseudospin singlet pairing takes over [18,29,31]. Therefore we expect the phase diagram, in the parameter space spanned by J/U and U/t, to be dominated by helical p-wave and singlet pairing states for physical band parameters describing Sr$_2$RuO$_4$, where interorbital hybridization between d_{xz} and d_{yz} orbitals can not be neglected. This expectation is confirmed by our RPA calculations, which give the phase diagram shown in Fig. 6. Details of the RPA calculation follow those found in Refs. [29,30]. The RPA breaks down for $U/t \gtrsim \mathcal{O}(1)$ due to an instability inherent in this approximation, [2] but can give reliable results even beyond the weak-coupling regime, $U/t \ll 1$ [38]. In Fig. 6, there is no trace of chiral pairing even at an intermediate value of J/U. In this phase diagram, the helical state order parameter realized is $\mathbf{d}(\mathbf{k}) = \hat{x}k_x + \hat{y}k_y$ (A_{1u}), and the s and $d_{x^2-y^2}$ wave order parameters belong to the irreducible representation A_{1g} and B_{1g}, respectively, of the D_{4h} group. However, they are not simple lowest harmonic functions, but are highly anisotropic, similar to those found in Refs. [18,29]. In each phase of the phase diagram, the ratio of the gap magnitude on different bands depends on both J/U and U/t. However, unlike

---

[2] The eigenvalue of the effective interaction in the Cooper pairing channel, λ, diverges where RPA breaks down and for Fig. 6, we cut off the phase diagram at $(t/U)^2|\lambda| = 0.2$. The boundary is insensitive to the choice of a cutoff [provided it is $\gtrsim \mathcal{O}(1)$], since λ diverges rapidly in this region

Ref. [18] where the $\alpha + \beta$ always dominate when the favored pairing symmetry is helical, we find that the dominant band in the helical phase is γ when both J/U and U/t are small, while it changes to $\alpha + \beta$ at larger J/U or U/t.

Since chiral p-wave pairing states have been previously found in various numerical calculations using the same model [18,24,29,30], we comment on these. In Ref. [24], the dominant pairing instability was calculated by solving Eliashberg equations with an effective pairing interaction derived from a perturbation theory up to second order in the bare interaction. Chiral p-wave was found to be the dominant channel when the Eliashberg equations were solved only for the γ band, while the coupling between γ and $\alpha + \beta$ bands due to the effective interaction was neglected. However, this coupling can have significant effects on the ratio between the gap magnitudes of the two sets of bands [18,29], which in turn can impact the relative stability between helical and chiral p-wave pairing states. This can explain the difference between our numerical results and those in Ref. [24]. Ref. [18] is a weak-coupling RG calculation, where chiral p-wave states have been found near $J/U = 0$ with a nonzero $t'''/t = 0.01$. However, this is inconsistent with our analytical analyses of the t''' effect in Sec. III C and also inconsistent with our numerical results in Fig. 6. Reference [29] is an RPA calculation based on the same model. The phase diagrams obtained in the weak-coupling limit are similar to those in Ref. [18]. In particular, there is a significant portion of the phase diagram at small J/U and U/t, where chiral p-wave pairing dominates. However, we note that Eq. (S13) of Ref. [29] takes the real part of the effective interaction. In the presence of SOC, this suppresses the t''' induced terms that we have identified in Eq. (15), which favors helical over chiral states. This may explain the discrepancy between our RPA phase diagram in Fig. 6 and those in Ref. [29]. In Ref. [30], a similar RPA calculation was performed at relatively large U for different Fermi surface geometries. Chiral p-wave pairing has been found only at large SOC for the Fermi surface geometry where the γ band touches the zone boundary. However, in that calculation, the interorbital hybridization t''' was set to zero, which completely leaves out the terms in Eq. (15). Physically we do not expect this hybridization to be vanishingly small, given that it is between orbitals on two next-nearest neighboring sites. Including a small $t''' = 0.01t$ suppresses the chiral p-wave pairing, giving way to helical states. We have verified this with RPA calculations in a parameter regime that overlaps with those of Ref. [30] and found results that are consistent with our analytical analysis. Furthermore, we find the stability of chiral p-wave in this parameter regime requires fine-tuning, in that a small change in parameters renders this phase unstable.

Given the difficulty of stabilizing a chiral p-wave state within the current model, we wonder what ingredients can favor a chiral p-wave state if we go beyond this model. There are at least two possibilities to consider: (1) three-dimensional effects on the normal state Fermi surface; (2) longer range off-site interactions.

In a 3D model with the same on-site Kanamori-Hubbard interaction, like the one used in Ref. [31], two additional interorbital hybridization terms appear in the normal state Hamiltonian, $t_{xz,xy}$ ($t_{yz,xy}$) between d_{xz} (d_{yz}) and d_{xy} orbitals,

in addition to the t''' that we have already considered. The two interlayer hybridizations $t_{xz,xy}$ and $t_{yz,xy}$, combined with the finite SOC, can mix an out-of-plane component $k_z(\hat{x}, \hat{y})$ in the $\mathbf{d}(\mathbf{k})$ vector of the chiral p-wave pairing state within the E_u representation [14,39,40], which shifts the T_c of the chiral p-wave state. However, this mixing is small because of its dependence on small parameters η/t and t_z/t, where $t_z \equiv \max\{|t_{yz,xy}|, |t_{xz,xy}|\}$. The mixing vanishes if either $\eta = 0$ or $t_z = 0$ so that, to leading order in η/t and t_z/t, it is $\propto \eta t_z/t^2$. The resulted critical temperature shift from the mixing can be estimated by a second order nondegenerate perturbation theory and the result is $\delta T_c/T_c \propto (\eta t_z/t^2)^2$. Detailed discussions can be found in Appendix C. This shift is negligible compared to the effects of other SOC induced terms on T_c that we discussed in Sec. III. Therefore we ignore the possible mixing in the following.

Then we can easily generalize our 2D analyses to the 3D model. If we set all interorbital hybridizations and J to zero, the same derivations as in Sec. III B lead to the same conclusion that all p-wave pairing states remain degenerate even with $\eta \neq 0$. Note that in this case there is no mixing between the in-plane and out-of-plane pairings because the full pseudospin SU(2) symmetry is still preserved. SOC induced terms by each interorbital hybridization can be analyzed similarly following Sec. III C. The two additional hybridizations, $t_{xz,xy}$ and $t_{yz,xy}$, add two additional terms to the $\delta \widetilde{H}_K(\mathbf{k})$ in Eq. (14) that are $\propto t_{xz,xy} \sin k_z/2 \cos k_x/2 \sin k_y/2 \cdots$ and $\propto t_{yz,xy} \sin k_z/2 \cos k_y/2 \sin k_x/2 \cdots$, respectively [31]. However, the leading order GL free energy from these two terms vanish in $\delta \mathcal{F} = \langle \delta \widetilde{H}_K(\mathbf{k}) \rangle$ after the $\mathbf{k}$ average, since we have ignored a possible mixing of the out-of-plane p_z pairing component, and the odd k_z dependence of those two terms can not be compensated by any other term in the mean field Hamiltonian of a p_x or p_y pairing state. Therefore, to linear order in $t_{xz,xy}/t$ or $t_{yz,xy}/t$, which are expected to be even smaller than t'''/t, we can drop those additional hybridizations in the normal state Hamiltonian. Then the analyses of the t''' and J induced terms are identical to those in Sec. III C and III D. Therefore the conclusions obtained in the 2D analysis can be directly applied to the 3D model. In other words, the three-dimensional effect of the FS does not help stabilize a chiral p-wave pairing state, consistent with the 3D weak-coupling RG numerical results obtained in Ref. [31], where helical states have been found to dominate over chiral p-wave pairing at J/U all the way up to $J/U = 0.2$.

Another possibility is to consider longer-range off-site interaction models [23,41]. Reference [23] considered such a model with attractive nearest neighbor interactions, and, indeed, chiral p-wave pairing states were found to be stabilized in some regime of the pairing interaction parameter space. However, the solutions were obtained under the assumption that the p-wave pseudospin triplet channel is favored over singlet channels. In Ref. [41], the authors studied a nearest neighbor version of the Kanamori-Hubbard interaction model, and found that p-wave pseudospin triplet states are more stable than singlet channels for certain choice of interaction parameters; on the other hand, the relative stability among different p-wave pairing states has been completely ignored by simply assuming that chiral p-wave pairing states are favored over helical states. In both cases, further investigations beyond

the assumptions made here would be needed to establish the stability of chiral *p*-wave states.

V. CONCLUSIONS

We have conducted a thorough study of the effect of SOC on the relative stability of different *p*-wave pairing states for a widely used microscopic model for Sr_2RuO_4. Our analysis combines a general GL free energy expansion with an analytical study of the symmetry of the microscopic model Hamiltonian. We give the most general form of the SOC induced quadratic GL terms that break the pseudospin SU(2) rotation symmetry, identify the relevant GL terms for the microscopic model, and examine their effects on lifting the degeneracy among different *p*-wave pairing states. The analytical results are further supported by our weak-coupling RG and RPA numerical calculations.

A theme that emerges from this study is that the breaking of SU(2) rotation symmetry in pseudospin space can be quite different from that in the actual spin space; this was also pointed out in Ref. [24]. The former depends on not only the presence of SOC but also other ingredients of the microscopic Hamiltonian, which in the current model are the interorbital hybridization t''', Hund's coupling J, and/or pair hopping. The additional dependence on t''' and J significantly reduces the splitting among different *p*-wave states for Sr_2RuO_4 since both t'''/t and J/U are small. In the parameter space regime relevant to Sr_2RuO_4, with finite but small t'''/t and small J/U, we find that the finite t''' effect tends to dominate and always stabilizes helical states over the chiral ones. We have also generalized our analysis to a 3D model and shown that the existence of interorbital hybridizations, in addition to the t''' that already exists in 2D models, does not help stabilize the chiral *p*-wave pairing states, in agreement with the recent numerical study [31]. On the other hand, including longer-range interactions may or may not make the chiral states more favorable and requires further investigation.

Our analysis has resolved some conflicts among different results on the relative stability between helical and chiral *p*-wave pairing states in the literature. Since the analysis is largely based on the symmetries of the model and independent of how the model is treated, it also serves as a guide for future studies, both analytical and numerical. Furthermore, the analysis presented here can be adapted to study the effect of SOC on other multiorbital pseudospin triplet superconductors.

An outstanding issue in Sr_2RuO_4 is to reconcile theory with the observations of broken time-reversal symmetry [1,3] and a jump in the shear modulus c_{66} [42]. Although a chiral *p*-wave state can explain both, here we discuss possible alternative explanations with helical states.

Given the small splitting among different helical states found here and in previous works [18,29,31,43], a possibility to consider is a pair of accidentally or nearly degenerate helical states. If the two states are close enough to degeneracy, such a pair can lead to either coexistence of different helical state domains [14,44] or a homogeneous time reversal breaking state [44–46], depending on microscopic interactions. A previous analysis of quartic GL terms [47] suggests that a homogeneous time reversal symmetry breaking state is almost impossible unless the system is very near or right at the degen-

eracy point. Moreover, except right at the degeneracy point, this scenario requires two phase transitions with different T_c, which is not observed experimentally. Nevertheless, if two almost degenerate helical orders do form a homogeneous state, this can lead to a jump in c_{66} if the two mixed representations are $\{A_{1u}, B_{2u}\}$ or $\{A_{2u}, B_{1u}\}$ [43]. However, within the models studied in this paper, our analysis in Sec. III suggests that residual symmetries in pseudospin space do not naturally lead to a degeneracy between A_{1u} (A_{2u}) and B_{2u} (B_{1u}).

In the case of coexistence of domains, time reversal breaking is possible at domain walls where two different helical order parameters coexist. However, since the order parameter mixing is local, the resulted coupling to external probes, such as light in a Polar Kerr measurement [3] and the shear strain ϵ_{xy} in an ultrasound measurement [42], is also local, which makes it unlikely to be able to account for the experiments. So a theoretical explanation of both broken time-reversal symmetry and a jump in c_{66} is highly constrained. Further investigations, both experimentally and theoretically, are needed to better assess the possibility of reconciling the experiments with helical ordered states.

Note added. Recently, Ref. [30] was updated with additional calculations on the effects of the interorbital hybridization t'''. Their new results are consistent with our analysis.

APPENDIX A: SOC INDUCED GL FREE ENERGY TERMS AT QUADRATIC ORDER FOR 2D MODELS

As mentioned in the main text, the remaining symmetry group in the presence of SOC is $D_{4h}^{\hat{L}+\hat{S}} \otimes U(1)^C$ for a 2D model. To derive all possible GL free energy terms at quadratic order for the pseudospin triplet pairing states, we contract the rank-4 tensor, $(d_i^\mu)^* d_j^\nu$, to a scalar such that it is invariant under all symmetry operations of the above group. For 2D models, the xy-plane mirror reflection symmetry of $D_{4h}^{\hat{L}+\hat{S}}$, denoted as $\mathcal{M}_{xy}^{\hat{S}}$, is operative only on the pseudospin since there is no k_z. $\mathcal{M}_{xy}^{\hat{S}}$ requires that, in $(d_i^\mu)^* d_j^\nu$, either $\{\mu, \nu\} = \{x, y\}$ or $\mu = \nu = z$.

For the case of $\{\mu, \nu\} = \{x, y\}$, there are only four possible independent contractions, given in Table III. With $\mu = \nu = z$ the only possible contraction is

$$\sum_{ij=\{x,y\}} \delta_{ij} \left(d_i^z\right)^* d_j^z = \left|d_x^z\right|^2 + \left|d_y^z\right|^2. \tag{A1}$$

Linear combinations of the four terms from Table III and the one in Eq. (A1) gives the five terms in Table I of the main text. The above SOC induced free energy terms can be also rewritten in terms of the order parameter matrix $\hat{\Delta}$. Rewriting

TABLE III. All possible contractions of $(d_i^\mu)^* d_j^\nu$ that are invariant under the $D_{4h}^{\hat{L}+\hat{S}} \otimes U(1)^C$ group for $\{\mu, \nu\} = \{x, y\}$. For 2D models, $\{i, j\} = \{x, y\}$.

Different contractions	Results
$\sum_{\mu\nu ij=\{x,y\}} \delta_{\mu i}\delta_{\nu j} (d_i^\mu)^* d_j^\nu$	$\sum_{ij=\{x,y\}} (d_i^i)^* d_j^j$
$\sum_{\mu\nu ij=\{x,y\}} \delta_{\mu j}\delta_{\nu i} (d_i^\mu)^* d_j^\nu$	$\sum_{ij=\{x,y\}} (d_i^j)^* d_j^i$
$\sum_{\mu\nu ij=\{x,y\}} \delta_{\mu\nu}\delta_{ij} (d_i^\mu)^* d_j^\nu$	$\sum_{ij=\{x,y\}} (d_i^j)^* d_i^j$
$\sum_{\mu\nu ij=\{x,y\}} \delta_{\mu i}\delta_{ij}\delta_{j\nu} (d_i^\mu)^* d_j^\nu$	$|d_x^x|^2 + |d_y^y|^2$

the five terms in Table I using Eq. (1) and linearly recombining them gives the five independent terms in Table IV, from which we see that order parameter products other than $\hat{\Delta}^\dagger \hat{\Delta}$, such as $\hat{\Delta}\sigma_i\hat{\Delta}$ and $\hat{\Delta}\sigma_i\hat{\Delta}\sigma_j$, also appear in the free energy expansion, due to the broken pseudospin SU(2) symmetry [34].

APPENDIX B: SOC DEPENDENCE OF THE SPLITTING BETWEEN HELICAL AND CHIRAL STATES WHEN $J = J' = 0$

The η dependence of $\delta\mathcal{F}$ for the 2D model at $J = J' = 0$ is calculated in weak-coupling RG and shown in Fig. 7. As mentioned in the main text, we find that the splitting between helical states has a quadratic dependence on η for small η at $J/U = 0$. This result can be understood as follows. When both $\eta = 0$ and $J' = J = 0$, the two-particle effective interaction has no coupling between $\alpha + \beta$ bands, which consist of the d_{xz} and d_{yz} orbitals, and the γ band, if only intraband pairing is considered as in the weak-coupling RG [18]. Then the pairing lives purely on the γ band since that band has a larger density of states. Therefore, at zero order in η, all the off-diagonal density matrices in Eq. (17) are identically zero. As a consequence, $\delta\mathcal{F} \sim \mathcal{O}(\eta^2)$. However, in general, we expect the three bands to be coupled even when $\eta = 0$ if the pair hopping $J' \neq 0$. In that case, $\delta\mathcal{F}$ picks up a linear in η term, as seen in Fig. 5. The η linear term is likely to dominate over the η^2 term since its estimated J/U for Sr$_2$RuO$_4$ is about 0.1 (see Ref. [18] and the references therein). Note that even a small J/U can strongly couple the three bands together such that order parameter magnitudes on the three bands are comparable [18]. This is largely because the normal state

TABLE IV. All possible SOC induced GL free energy terms at quadratic order in $\hat{\Delta}$ for the pseudospin triplet pairing states in a 2D model. $\hat{\Delta}_x$ is the part of the order parameter matrix $\hat{\Delta}$ that transforms like k_x under the spatial D_{4h} group. The trace Tr is performed in the pseudospin space. Note that, in this table, $f_2^{\text{SOC},E}$ is allowed because the pseudospin Pauli matrix σ_z is even under the xy-plane mirror reflection $\mathcal{M}_{xy}^{\hat{S}}$.

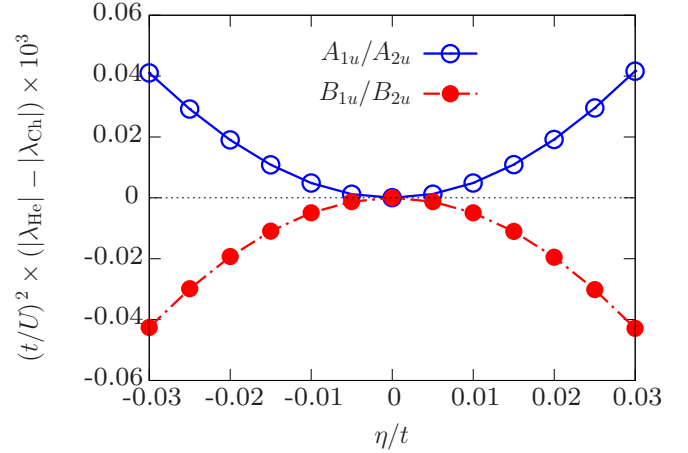| GL terms	Expressions in terms of $\hat{\Delta}$
$f_2^{\text{SOC},A}$	$\text{Tr}[\hat{\Delta}_x^\dagger \sigma_z \hat{\Delta}_x \sigma_z] + \text{Tr}[\hat{\Delta}_y^\dagger \sigma_z \hat{\Delta}_y \sigma_z]$
$f_2^{\text{SOC},B}$	$\text{Tr}[\hat{\Delta}_y^\dagger \sigma_x \hat{\Delta}_y \sigma_x] - \text{Tr}[\hat{\Delta}_x^\dagger \sigma_y \hat{\Delta}_x \sigma_y]$
$f_2^{\text{SOC},C}$	$\text{Tr}[\hat{\Delta}_x^\dagger \sigma_x \hat{\Delta}_x \sigma_x] - \text{Tr}[\hat{\Delta}_y^\dagger \sigma_y \hat{\Delta}_y \sigma_y]$
$f_2^{\text{SOC},D}$	$\text{Tr}[\hat{\Delta}_x^\dagger \sigma_x \hat{\Delta}_y \sigma_y] - \text{Tr}[\hat{\Delta}_y^\dagger \sigma_y \hat{\Delta}_x \sigma_x]$
$f_2^{\text{SOC},E}$	$i\{\text{Tr}[\hat{\Delta}_x^\dagger \sigma_z \hat{\Delta}_y] - \text{Tr}[\hat{\Delta}_y^\dagger \sigma_z \hat{\Delta}_x]\}$

FIG. 7. η/t dependence of the splitting between helical and chiral p-wave pairing states in weak-coupling RG. $t''' = 0.1t$ and $J = 0$. The splittings are $\propto (\eta/t)^2$ to leading order in η.

density of states of the $\alpha + \beta$ bands is comparable to that of the γ band.

APPENDIX C: SOC INDUCED GL FREE ENERGY TERMS AT QUADRATIC ORDER FOR 3D MODELS

For a 3D model that depends on k_z, in addition to the basis functions given in Table II, an out-of-plane pairing component, with the basis function $\mathbf{d}(\mathbf{k}) = \hat{z}k_z$ for the A_{1u} and $\mathbf{d}(\mathbf{k}) = k_z(\hat{x}, \hat{y})$ for the E_u representation, is also allowed by symmetry [14,39,40]. In the presence of SOC and interlayer coupling, in general, the vector $\mathbf{d}(\mathbf{k})$ of the E_u (but not the A_{1u}; see below) representation is a mixture of the in-plane and out-of-plane pairing components, which leads to more GL free energy terms at quadratic order in $\hat{\Delta}$.

To obtain these GL free energy terms, we follow the 2D derivations outlined in Appendix A. The only difference is that, for 3D models, the xy-plane mirror reflection, $\mathcal{M}_{xy}^{\hat{L}+\hat{S}}$, now operates on both the $\mathbf{k}$ and pseudospin. Besides the terms in Table I, we also get

$$f_2^{\text{SOC},6} = |d_z^z|^2, \tag{C1a}$$

$$f_2^{\text{SOC},7} = |d_z^x|^2 + |d_z^y|^2, \tag{C1b}$$

$$f_2^{\text{SOC},8} = \sum_{j=\{x,y\}} [(d_j^z)^* d_z^j + \text{c.c.}], \tag{C1c}$$

$$f_2^{\text{SOC},9} = \sum_{j=\{x,y\}} i[(d_j^z)^* d_z^j - \text{c.c.}]. \tag{C1d}$$

$f_2^{\text{SOC},6}$ and $f_2^{\text{SOC},7}$ describe the free energy contributions from the $\mathbf{d}(\mathbf{k}) = \hat{z}k_z$ and $\mathbf{d}(\mathbf{k}) = k_z(\hat{x}, \hat{y})$ pairings, respectively. They exist even without SOC. However, $f_2^{\text{SOC},6}$ and $f_2^{\text{SOC},7}$ are irrelevant to our current discussions since the T_c of the out-of-plane pairings are expected to be much smaller than that of the in-plane components for Sr$_2$RuO$_4$, which is highly quasi-2D. The other two GL terms, $f_2^{\text{SOC},8}$ and $f_2^{\text{SOC},9}$, describe the coupling between the in-plane $\mathbf{d}(\mathbf{k}) = \hat{z}(k_x, k_y)$ and out-of-plane $\mathbf{d}(\mathbf{k}) = k_z(\hat{x}, \hat{y})$ components within the same

E_u representation. Their appearance requires finite SOC to break the full psedospin rotational symmetry. Note that such a coupling does not exist for the A_{1u} representation.

The mixing of the out-of-plane component to the in-plane chiral p-wave pairing state in E_u leads to a shift of the T_c away from its zero SOC value, T_c^0. On the other hand, the helical p-wave states are unaffected by the mixing; therefore, the degeneracy among different p-wave states is in general lifted due to the shift. Hence it is important to understand the magnitude of this shift, and compare it to the effect of other SOC induced GL terms on T_c that we have discussed in Sec. III of the main text.

To that end, we first analyze the dependence of the GL coefficients associated with $f_2^{SOC,8}$ and $f_2^{SOC,9}$, a_8 and a_9, on small parameters of the model that we consider [31]. Spin rotation symmetry breaking requires that, to leading order in η, $\{a_8, a_9\} \propto \eta/t$. Since the terms in $f_2^{SOC,8}$ and $f_2^{SOC,9}$ transform like $k_x k_z$ or $k_y k_z$ under spatial rotations, the two GL coefficients necessarily come from a **k** space average $\langle \cdots k_x k_z \rangle$ or $\langle \cdots k_y k_z \rangle$, which is nonzero only if the $k_x k_z$ or $k_y k_z$ dependence is compensated by interlayer hopping terms such as $t_{yz,xy} \sin k_x/2 \sin k_z/2 \cos k_y/2$ or $t_{xz,xy} \sin k_y/2 \sin k_z/2 \cos k_x/2$. As a consequence, to leading order in $t_{yz,xy}/t$ and $t_{xz,xy}/t$, $\{a_8, a_9\} \propto t_z/t$, where $t_z = \max\{|t_{yz,xy}|, |t_{xz,xy}|\}$. Combing the η/t and t_z/t dependence, we have $\{a_8, a_9\} \propto T_c^0(\eta \, t_z)/t^2$, where T_c^0 is a characteristic pairing temperature scale for zero SOC.

Now consider the T_c shift of the chiral p-wave pairing state due to the mixing. As mentioned above, we expect that, for Sr$_2$RuO$_4$, the T_c of the in-plane and out-of-plane pairing components in the E_u representation, $T_{c,\text{in}}$ and $T_{c,\text{out}}$, satisfy $T_{c,\text{in}} \gg T_{c,\text{out}}$. So the T_c shift of the in-plane chiral p-wave pairing state due to the mixing can be well estimated from a second order non-degenerate perturbation theory, i.e., $\delta T_c \approx \max\{|a_8|^2, |a_9|^2\}/(T_{c,\text{in}} - T_{c,\text{out}})$, which leads to $\delta T_c/T_c \propto (\eta \, t_z)^2/t^4$. This shift is negligible compared with the contributions from other SOC induced terms that we have discussed in the main text, since $\eta/t \sim 0.1$ and $|t_z/t| \lesssim 0.1$ for Sr$_2$RuO$_4$.

[1] G. Luke, Y. Fudamoto, K. Kojima, M. Larkin, J. Merrin, B. Nachumi, Y. Uemura, Y. Maeno, Z. Mao, Y. Mori *et al.*, Nature (London) **394**, 558 (1998).

[2] K. Ishida, H. Mukuda, Y. Kitaoka, K. Asayama, Z. Mao, Y. Mori, and Y. Maeno, Nature (London) **396**, 658 (1998).

[3] J. Xia, Y. Maeno, P. T. Beyersdorf, M. M. Fejer, and A. Kapitulnik, Phys. Rev. Lett. **97**, 167002 (2006).

[4] A. P. Mackenzie and Y. Maeno, Rev. Mod. Phys. **75**, 657 (2003).

[5] C. Kallin and J. Berlinsky, Rep. Prog. Phys. **79**, 054502 (2016).

[6] A. J. Leggett, Rev. Mod. Phys. **47**, 331 (1975).

[7] N. Read and D. Green, Phys. Rev. B **61**, 10267 (2000).

[8] C. Nayak, S. H. Simon, A. Stern, M. Freedman, and S. Das Sarma, Rev. Mod. Phys. **80**, 1083 (2008).

[9] A. P. Mackenzie, T. Scaffidi, C. W. Hicks, and Y. Maeno, Quantum Materials **2**, 40 (2017).

[10] M. Matsumoto and M. Sigrist, J. Phys. Soc. Jpn. **68**, 994 (1999).

[11] J. R. Kirtley, C. Kallin, C. W. Hicks, E.-A. Kim, Y. Liu, K. A. Moler, Y. Maeno, and K. D. Nelson, Phys. Rev. B **76**, 014526 (2007).

[12] C. W. Hicks, D. O. Brodsky, E. A. Yelland, A. S. Gibbs, J. A. N. Bruin, M. E. Barber, S. D. Edkins, K. Nishimura, S. Yonezawa, Y. Maeno, and A. P. Mackenzie, Science **344**, 283 (2014).

[13] A. Steppke, L. Zhao, M. E. Barber, T. Scaffidi, F. Jerzembeck, H. Rosner, A. S. Gibbs, Y. Maeno, S. H. Simon, A. P. Mackenzie, and C. W. Hicks, Science **355**, eaaf9398 (2017).

[14] A. Pustogow, Y. Luo, A. Chronister, Y.-S. Su, D. Sokolov, F. Jerzembeck, A. Mackenzie, C. Hicks, N. Kikugawa, S. Raghu *et al.*, Nature (London) **574**, 72 (2019).

[15] K. Ishida, M. Manago, and Y. Maeno, arXiv:1907.12236.

[16] M. W. Haverkort, I. S. Elfimov, L. H. Tjeng, G. A. Sawatzky, and A. Damascelli, Phys. Rev. Lett. **101**, 026406 (2008).

[17] A. Tamai, M. Zingl, E. Rozbicki, E. Cappelli, S. Riccò, A. de la Torre, S. McKeown Walker, F. Y. Bruno, P. D. C. King, W. Meevasana, M. Shi, M. Radović, N. C. Plumb, A. S. Gibbs, A. P. Mackenzie, C. Berthod, H. U. R. Strand, M. Kim, A. Georges, and F. Baumberger, Phys. Rev. X **9**, 021048 (2019).

[18] T. Scaffidi, J. C. Romers, and S. H. Simon, Phys. Rev. B **89**, 220510(R) (2014).

[19] H. S. Røising, F. Flicker, T. Scaffidi, and S. H. Simon, Phys. Rev. B **98**, 224515 (2018).

[20] D. F. Agterberg, T. M. Rice, and M. Sigrist, Phys. Rev. Lett. **78**, 3374 (1997).

[21] M. Sigrist, D. Agterberg, A. Furusaki, C. Honerkamp, K. Ng, T. Rice, and M. Zhitomirsky, Physica C (Amsterdam) **317-318**, 134 (1999).

[22] K.-K. Ng and M. Sigrist, Physica B (Amsterdam) **281-282**, 969 (2000).

[23] K. K. Ng and M. Sigrist, Europhys. Lett. **49**, 473 (2000).

[24] Y. Yanase and M. Ogata, J. Phys. Soc. Jpn. **72**, 673 (2003).

[25] J. F. Annett, G. Litak, B. L. Györffy, and K. I. Wysokiński, Phys. Rev. B **73**, 134501 (2006).

[26] S. Raghu, A. Kapitulnik, and S. A. Kivelson, Phys. Rev. Lett. **105**, 136401 (2010).

[27] C. M. Puetter and H.-Y. Kee, Europhys. Lett. **98**, 27010 (2012).

[28] Y. Yanase, S. Takamatsu, and M. Udagawa, J. Phys. Soc. Jpn. **83**, 061019 (2014).

[29] L.-D. Zhang, W. Huang, F. Yang, and H. Yao, Phys. Rev. B **97**, 060510(R) (2018).

[30] A. T. Rømer, D. D. Scherer, I. M. Eremin, P. J. Hirschfeld, and B. M. Andersen, Phys. Rev. Lett. **123**, 247001 (2019).

[31] H. S. Røising, T. Scaffidi, F. Flicker, G. F. Lange, and S. H. Simon, Phys. Rev. Res. **1**, 033108 (2019).

[32] Q. H. Wang, C. Platt, Y. Yang, C. Honerkamp, F. C. Zhang, W. Hanke, T. M. Rice, and R. Thomale, Europhys. Lett. **104**, 17013 (2013).

[33] W.-S. Wang, C.-C. Zhang, F.-C. Zhang, and Q.-H. Wang, Phys. Rev. Lett. **122**, 027002 (2019).

[34] D. Vollhardt and P. Wolfle, *The Superfluid Phases of Helium 3* (Taylor & Francis, 1990).

[35] A. Georges, L. d. Medici, and J. Mravlje, Annu. Rev. Condens. Matter Phys. **4**, 137 (2013).

[36] W. Kohn and J. M. Luttinger, Phys. Rev. Lett. **15**, 524 (1965).

[37] Y. Imai, K. Wakabayashi, and M. Sigrist, Phys. Rev. B **85**, 174532 (2012).

[38] A. T. Rømer, T. A. Maier, A. Kreisel, I. Eremin, P. J. Hirschfeld, and B. M. Andersen, arXiv:1909.00627.

[39] M. Sigrist and K. Ueda, Rev. Mod. Phys. **63**, 239 (1991).

[40] W. Huang and H. Yao, Phys. Rev. Lett. **121**, 157002 (2018).

[41] S. Koikegami, Y. Yoshida, and T. Yanagisawa, Phys. Rev. B **67**, 134517 (2003).

[42] C. Lupien, Ultrasound attenuation in the unconventional superconductor Sr_2RuO_4, Ph.D. thesis, University of Toronto, 2002; S. Ghosh, A. Shekhter, F. Jerzembeck, N. Kikugawa, D. A. Sokolov, A. P. Mackenzie, C. W. Hicks, and B. J. Ramshaw (unpublished).

[43] A. Ramires and M. Sigrist, Phys. Rev. B **100**, 104501 (2019).

[44] M. Khodas and A. V. Chubukov, Phys. Rev. Lett. **108**, 247003 (2012).

[45] D. F. Agterberg, V. Barzykin, and L. P. Gor'kov, Phys. Rev. B **60**, 14868 (1999).

[46] V. Stanev and Z. Tešanović, Phys. Rev. B **81**, 134522 (2010).

[47] W. Huang, T. Scaffidi, M. Sigrist, and C. Kallin, Phys. Rev. B **94**, 064508 (2016).